



BERYLLIUM BRAZING CONSIDERATIONS IN CANDU FUEL BUNDLE MANUFACTURE

J.G. Harmsen^{*1}, B.J. Lewis², A. Pant¹ and W.T. Thompson²

¹ Cameco Fuel Manufacturing

^{*}(200 Dorset Street East Port Hope, On L1A 3V4, 905-885-4537ext2338)

² Department of Chemistry and Chemical Engineering,
Royal Military College of Canada, Kingston, Ontario, Canada

ABSTRACT

At Cameco Fuel Manufacturing (CFM), appendages are currently joined to fuel bundle elements by vacuum beryllium brazing. Recent indications of a future reduction of the Ontario Environmental Limit on airborne beryllium particles, combined with the continuous efforts by CFM on process and product improvements, initiated this study to find a substitute for pure beryllium.

The presentation will review the necessary functionality of brazing alloy components and short list a series of alloys with the potential to duplicate the performance of pure beryllium. Modifications to the brazing process based on in-plant testing will be discussed in relation to the use of these alloys. The presentation will conclude with a summary of the progress to date and further testing expected to be necessary.

1. Introduction

Appendages such as spacers and bearing pads are brazed with beryllium onto the sheathing of fuel elements in the CANDU fuel bundle as part of the manufacturing operation at CFM. Airborne beryllium particles that may be generated during the production process are a potential hazard for operators. Exposure of operators is controlled via fixed location air monitors, engineering controls, safe work instructions, housekeeping procedures and personal protective equipment.

The American Conference of Governmental Industrial Hygienists® (ACGIH) has recently adopted a new Threshold Limit Value® Time Weighted Average (TLV-TWA) for occupational exposure to airborne beryllium. The new TWA of $0.05 \mu\text{g}/\text{m}^3$, for inhalable particles that are 100 microns in size and below replaces the currently practiced TWA limit of $2.0 \mu\text{g}/\text{m}^3$ of total airborne particulate.

The new TWA was introduced because:

- Beryllium is increasingly being used outside of the traditional high-technology industries;
- The amount of people exposed to beryllium worldwide has increased significantly;
- Cases of Beryllium Sensitization (BeS) and Chronic Beryllium Disease (CBD) were on the rise even though exposure levels remained below the previous $2.0 \mu\text{g}/\text{m}^3$ TWA limit.



The Ontario Ministry of Labor (MOL) adopts many of the ACGIH chemical TLV's into its legislation and in July 2009 had proposed to adopt the new beryllium TLV-TWA. MOL has held off legislating the new standard for now, but it is only a matter of time before the new standard is adopted.

To utilize this opportunity before legislation is passed, CFM collaborated with the Department of Chemistry and Chemical Engineering (Nuclear Physics Engineering) of the Royal Military College (RMC) in a joint effort as an initial proactive step for a project to investigate the reduction and/or elimination of beryllium airborne particles within the production facilities at CFM. Both institutions realized the importance of this matter to guarantee future fuel supply to CANDU reactors.

This project focuses on two issues: (i) the reduction of airborne beryllium particles, and (ii) the quest to find a suitable substitute for beryllium as a brazing component. This paper will address both.

Substitution of beryllium within the braze-joint will have both positive and negative effects on the product and processes upstream and downstream of the brazing operation. All possible effects need to be identified, quantified, measured and benchmarked against current practice to ensure the quality of the new designed braze-joint. This paper is therefore structured accordingly in the following sections: Process variables (Section 2), Braze properties (Section 3), Braze requirements (Section 4) and Customer requirements (Section 5).

The beryllium braze-joint design has been in use for over 40 years of reactor operation, with no significant braze-joint manufacturing or reactor safety issues. Improving on this braze-joint performance benchmark within the project is an extremely challenging objective.

2. Process variable: Airborne Beryllium particle levels

In order to determine the current state of the operation, 480 beryllium concentration values taken over the first 25 weeks of 2009 were analyzed. The data shows that exposure values are well below the current TWA of $2.0 \mu\text{g}/\text{m}^3$ airborne Be particles. However, if this data is compared with the new standard of $0.05 \mu\text{g}/\text{m}^3$, a reject level of 10% is observed. Because the data is not normal-distributed as shown in figure 1, the predicted reject level is slightly higher estimated at a value of 12%.

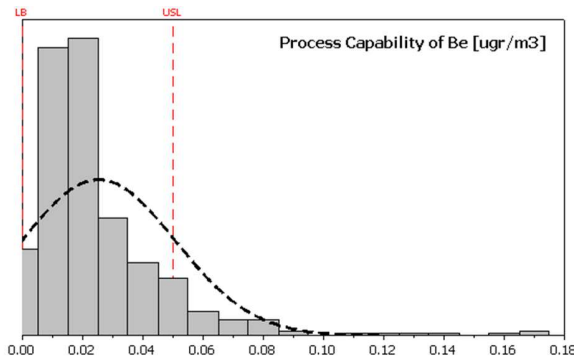


Figure 1 Capability of Be particles

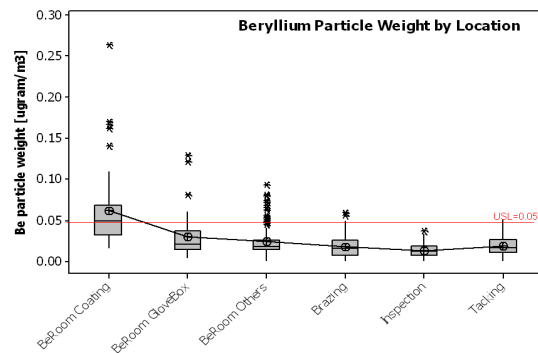


Figure 2 Be particles by process

Because the new TWA standard only accounts for inhalable particles smaller than $100 \mu\text{m}$ in size, the current measurement method may not be appropriate to compare the actual values with the given standard. For the purpose of this project, this method can still be used to determine whether significant Be particle reductions are realized. When the new TWA standard is imposed, re-calibration of the measuring system will be necessary in order to compensate for particle size variances.

Further analysis of the data (AnoVa-graph presented in figure 2) shows that the sample locations at the Be coating equipment picks up significantly more Be-particles than in any other process. This finding provided guidance for the strategy in the current project for the reduction of Be levels. It is believed that the Be airborne particles are mainly created after beryllium vaporization and sublimation within the CFM production process. This is addressed as an important area of investigation in the next section.



3. Braze properties

3.1. Vapor pressure-temperature curve of beryllium

Beryllium vapor is created out of the vaporization of its liquid phase and of the sublimation of the beryllium α -solid and β -solid phases. With the use of the a thermodynamic software package, the Be phase equilibrium can be established as function of temperature and partial pressure. This equilibrium is established when the Gibbs free energy of the phase transition is zero ($\Delta G=0$).

$$\Delta G_{\text{transition}} = \Delta G_{\text{gas}} - \Delta G_{\text{liquid, } \alpha\text{-solid, } \beta\text{-solid}} = 0 \text{ [J/mole]} \quad (1)$$

Each phase Gibbs free energy level is dependent on its thermodynamic properties of enthalpy (H) and entropy (S), which are functions of temperature (T) and pressure (P):

$$\Delta G_{T,P} = H^0_{T,P} - T \cdot S_{T,P} \quad (2)$$

All phase transition curves (see figure 3) are determined with software, which contains a database of thermodynamic properties with more than 4000 components and their phases. The intersections of the curves represent the triple points of the different phases.

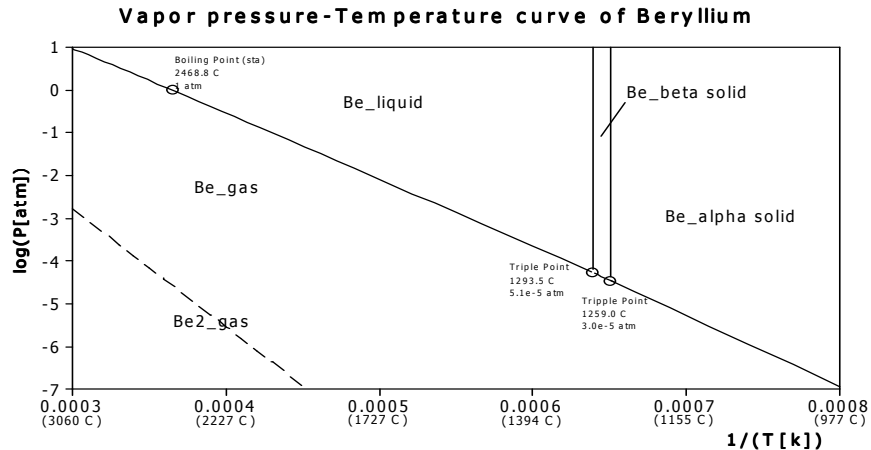


Figure 3 Vaporization curve of beryllium

The curves follow the Clausius-Clapyron equation:

$$d \ln(P)/d(1/T) = - \Delta H^{L \rightarrow V} / R = \text{Constant} \quad (3)$$

This equation shows that the (natural) logarithm of the pressure is linear dependent on the inverse temperature of the liquid. The partial pressure of the vaporizing material is not influenced



by the total pressure of the system. The Clausius-Clapyron equation is also applicable for other phase transitions.

The formation of Be₂ gas is also studied, but this concentration is 1000-10,000 times smaller than the Be gas concentration and this constituent is therefore not further considered.

3.2. Beryllium Zirconium binary phase system

Within the project, the thermodynamic properties of the beryllium and zirconium components are provided in the software database, as well as their solutions and phases. As such, a thermodynamic computation can be performed using a fundamental Gibbs energy minimization in order to develop a “model” of the reported phase diagram. With this model, within a certain level of precision, the beryllium partial vapor pressure can be calculated for each position on this diagram.

The latest study of the Be-Zr system originates from the work in 1987 as performed by Okamoto, Tanner and Abriata. The binary Be-Zr phase diagram is established from several previous studies and measurements of thermodynamic properties.

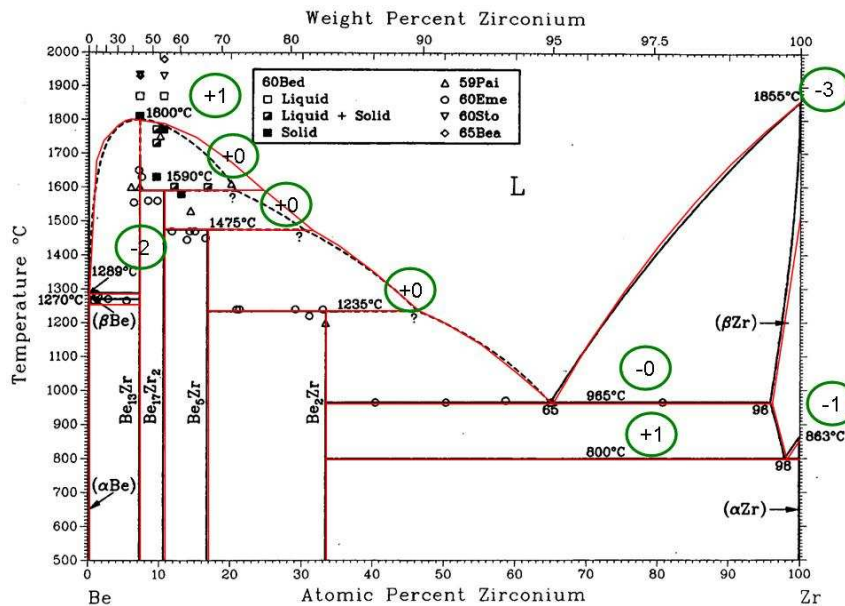


Figure 4 Evaluation of Be-Zr phase diagram

Figure 4 shows the original phase diagram by Okamoto and the superimposed thermodynamics model shown in red. Any difference in critical temperatures between the two representations is



shown as green encircled numbers. The main discrepancy is found in the upper right area of the diagram where the α -Zr rich Be solution does not ‘reach’ a melting point of 1865°C. Because this data is not relevant in the current analysis, no further effort was made to improve the model. This is also the case for the deviations in the upper left area of the diagram. Here Okamoto indicated a dotted line to indicate that such values were only an estimation.

The phase diagram is based on the combinations of Gibbs free energies of all the solutions, mixtures and compounds. Those energy curves are mapped for the eutectic temperature in figure 5.

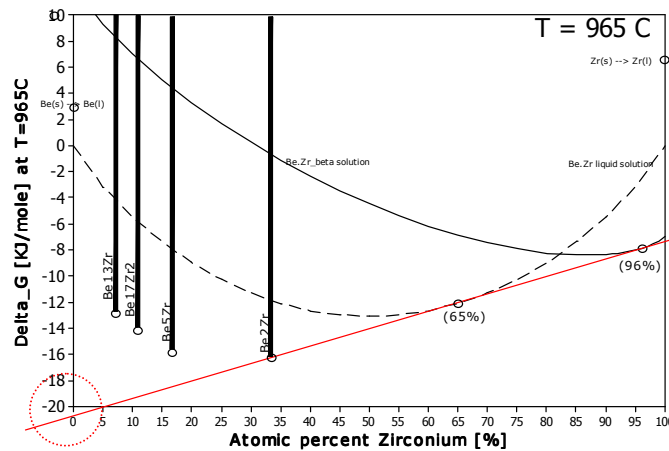


Figure 5 Gibbs free energy curves at T=965C

The red line in figure 5 shows the ‘common tangent rule’, which states that ‘the composition of two coexisting equilibrium phases lie at the points of common tangency of the free energy curve’. The common tangency, in this example applicable for three points, is expressed in the following formula.

$$D(G_{\text{BeZr}})/d(X_{\text{Zr}}) = d(G_{\text{Be-Zr liquid solution}})/d(X_{\text{Zr}}) = d(G_{\text{Zr rich } \beta\text{-solid solution}})/d(X_{\text{Zr}}) \quad (4)$$

It explains the existence of a mixture between 33% and 65% and a mixture between 65% and 96% atomic Zr percentage. Non-bounded beryllium atoms present within these two mixtures must be positioned on the same line for coexistence and can be found as the intersect of the line and vertical axis ($X_{\text{Be}}=100\%$), with a Gibbs free energy of -21 kJ/mol. With the use of formula 5 and the sublimation transition Gibbs free energy at 965°C (1 atm.) of 168 kJ/mol (see formula 1), the partial pressure of Be is calculated as 1.1×10^{-8} atm.

$$\Delta G_{\text{Be}} = R.T. \ln(P_{\text{Be}}/1) \quad (5)$$

This partial pressure is constant within a mixture and can be calculated in a similar fashion for all points in the phase diagram leading to the complete figure 6.

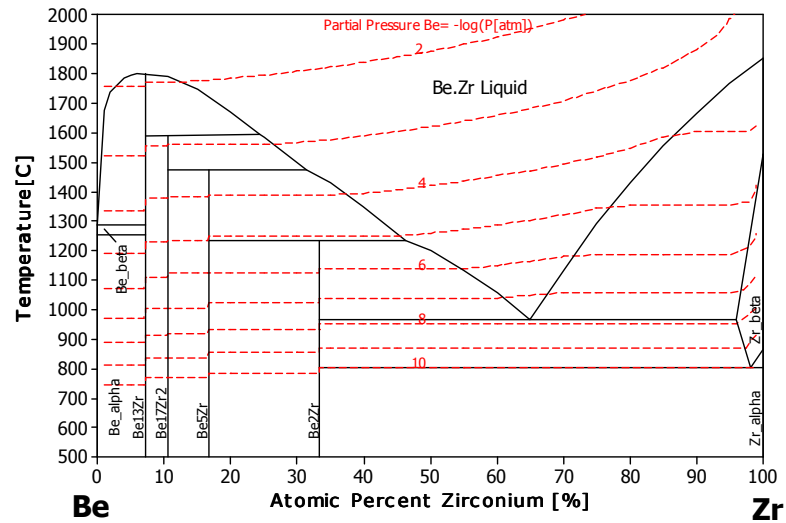


Figure 6 Be-Zr phase diagram with Be vaporization pressures

3.3. Metallurgical properties

Within the CFM production, there is an optical evaluation of braze-joint properties, which include: an observation of pitting, incomplete welds and Be-migration. Also performed is a microscopic evaluation with measurements of: the grain size, braze penetration depth, grain counts in the sheath and void length.



Figure 7 Optical evaluation

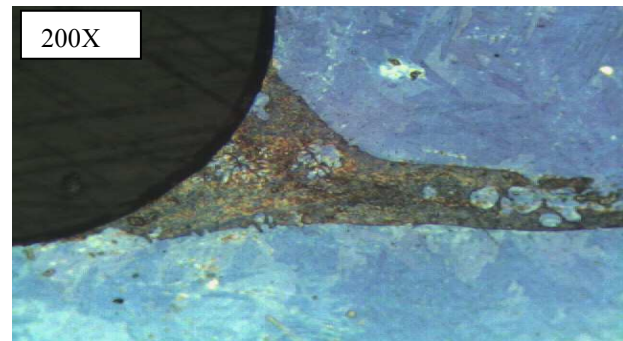


Figure 8 Microscopic evaluation

Historical data of these beryllium braze-joint properties will be used as benchmarks for the evaluation of other braze materials.

4. Braze Requirement

4.1. Mechanical strength

Due to the limited height of the bearing pad, an indirect shear tensile strength measurement was developed in order to evaluate the strength of the joint. A lower tube fixture holds the tube and exposes the bearing pad. An upper fixture fits over the bearing pad and a calibrated torque wrench is used to register the maximum torque needed to shear the bearing pad from the sheath (see figure 9).

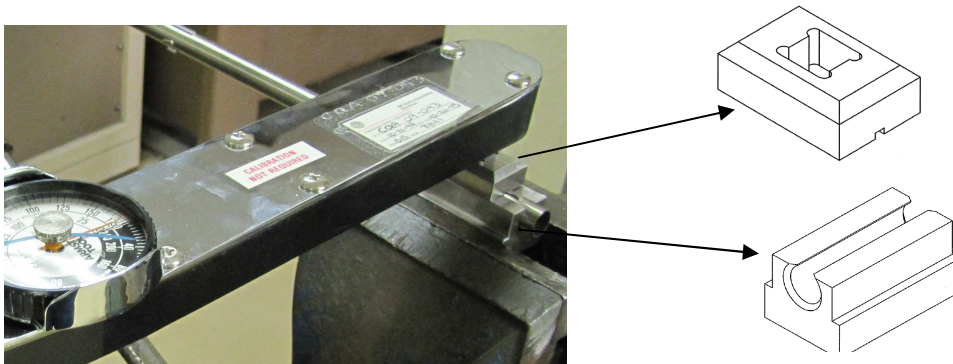


Figure 9 Torque test tube fixtures

In 98% of the cases examined, the bearing pad did not shear from the joint but rather from the surrounding sheath as shown in figure 10. The 50 measurements, which reveal a normal distribution with a value of 68 ± 6 N.m (for two standard deviations), are not representative of the joint strength but rather of the heat affective zone (HAZ) around the braze joint as depicted in figure 10.

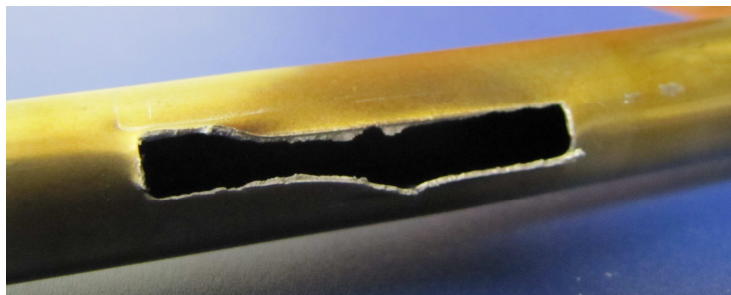


Figure 10 Sheared sheet after torque test

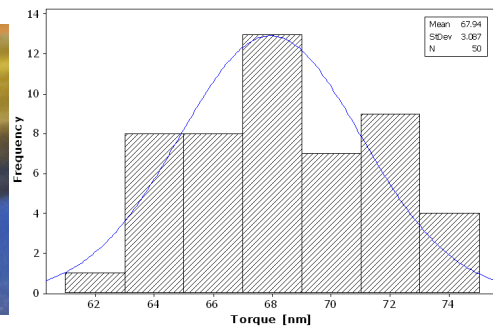


Figure 11 Torque distribution

The test findings suggest that more strength is not needed, and that less temperature impact during the joining process is recommended. The option of welding, as opposed to a joining process to replace brazing, was not considered in this project.

4.2. De-oxidation of zirconium oxide

Braze material should ‘wet’ the zirconium base material. This implies that it should form compounds with Zr and be able to access this Zr material by breakdown of the thin ZrO₂ passivating layer which protects the Zr. An Ellingham Oxidation diagram gives insight into the Gibbs free energy levels concerning different metal oxidation reactions. It reveals that the formation of ZrO₂ occurs at a relatively low Gibbs free energy level of -255 kJ/mol, making the selection of a de-oxidant limited. Practical de-oxidizing elements are: Sr, Li, Mg, Be, Ca, and Lanthanides such as La and Ce.

Phase diagram investigations show that none of the listed elements form compounds with Zr and have an eutectic temperature between 600-1100°C, with the exception of Be. Be combines both brazing functions in one element. This makes Be unique in its application and most likely the reason for its initial selection as a brazing material. Be alternatives must therefore consist of an alloy in which the main element makes compounds with Zr and the other component must be one of the listed de-oxidants. With the use of thermodynamic software, several Zr de-oxidation reactions were studied as shown in comparison in figure 12.

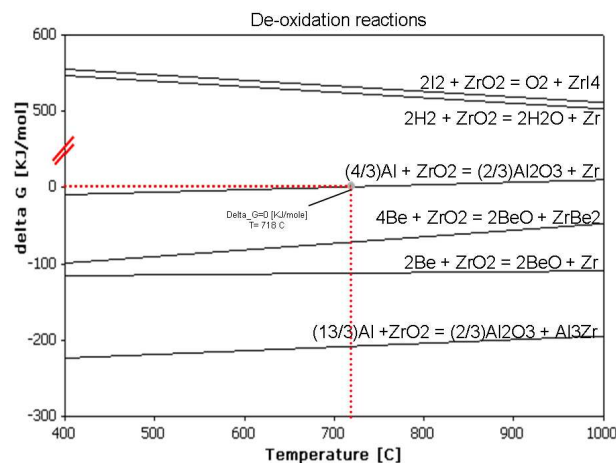


Figure 12 Gibbs free energy curves for different ZrO₂ reactions

Iodine and Hydrogen de-oxidation reactions show large positive free Gibbs energy levels indicating that the reactions will not spontaneously take place. The thin ZrO₂ layer is protective against these elements.

The Aluminum de-oxidation reaction of Zr has a Gibbs free energy around zero and is a marginal de-oxidizer. The AlZr phase diagram shows that Al forms several compounds with Zr and like Be, Al might have the two required brazing properties within one element. After determining the AlZr thermodynamic properties of solutions and compounds in a similar matter as described in section 3.2 (see figure 13), the de-oxidation reaction, with the compound of Al₃Zr included, yielded a better result (i.e., lower Gibbs free energy levels) than the de-oxidation reaction for Be (see figure 12).

In fact, experiments with Al foil as a brazing material within the CFM production environment resulted in several successful bearing pad-sheath braze-joints as shown in figure 14.

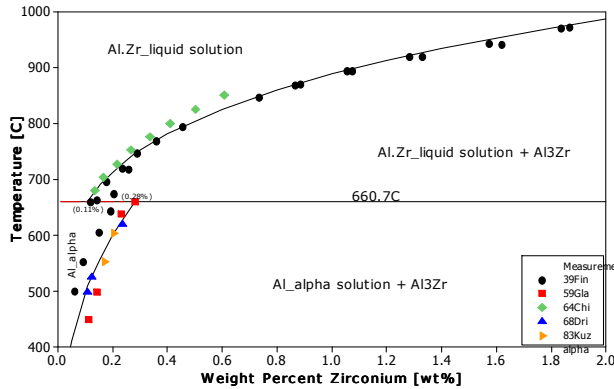


Figure 13 Evaluation of Al-Zr phase diagram

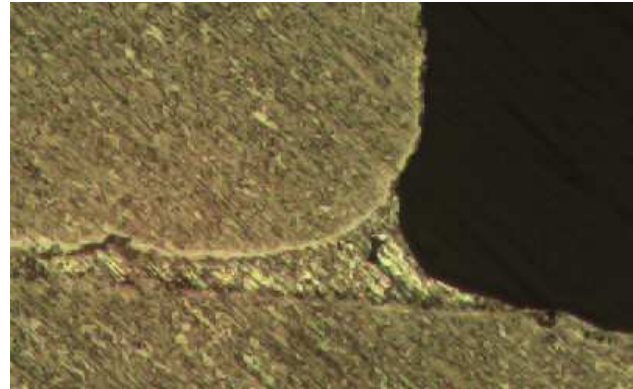


Figure 14 AlZr braze-joint (200X)

Although the braze is not completely fused like a Be braze, the Al de-oxidized the ZrO_2 layer and reacted with the Zr base material. ‘Wetting’ took place up to the sides of the bearing pad. More experiments, however, need to be performed to model the kinetic behavior of the fusing process.

5. Customer Requirement: Braze behavior in reactor environment

Within the operation of CANDU reactors, neutron absorption (/activation) of various in-core materials is very important.

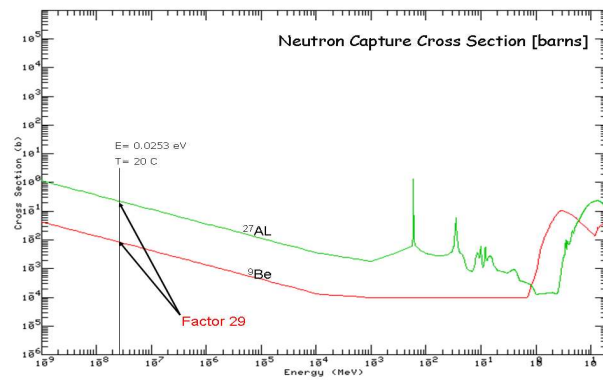


Figure 15 Neutron capture cross section of Be and Al

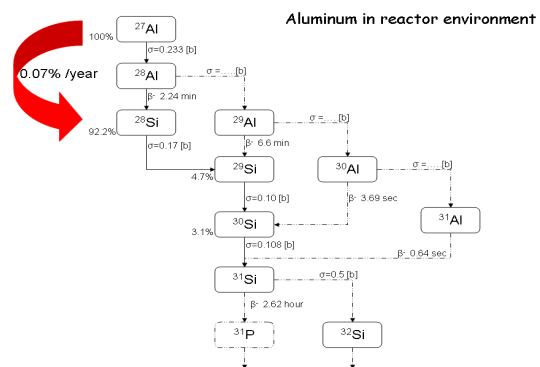


Figure 16 Al radiation stability



Be is one of the materials with the lowest neutron capture cross section and is even preferable above Zr (5 times lower cross section). Figure 15 shows that for thermal neutrons the absorption of Be is 29 times lower than for Al absorption.

Aluminum is relatively stable within the reactor. Natural (100%) ²⁷Al will absorb neutrons as indicated above and form ²⁸Al which decays (β⁻ decay) to natural (92%) ²⁸Si. The Si will eventually decay to P in four decay steps, which most likely will not happen during the lifetime of the fuel in the reactor. The transformation from Al to Si will happen at a rate of 0.07% per year based on the following activation equation.

$$N_{Si}/N_{Al} = 100\% \times \sigma_{27Al} \times \Phi \times \{t + (1 - e^{-\lambda_{28Al} \times t}) / \lambda_{28Al}\} \quad (6)$$

The concentration ratio of Si versus Al (N_{Si}/N_{Al}) is determined as function of the cross sections of ²⁷Al (σ) and the decay constant of ²⁸Al (λ). The neutron flux (Φ) is set to an average CANDU reactor flux of 1.02×10^{14} n.cm⁻².s⁻¹. The Si/Al ratio is graphed against reactor time (t expressed in years) in figure 17 for two different levels of neutron flux.

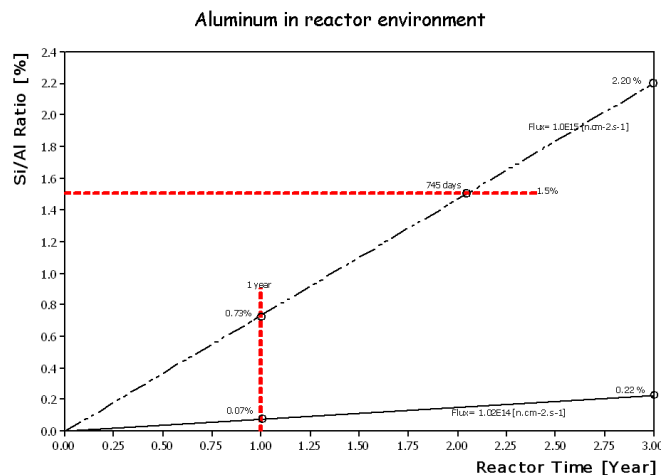


Figure 17 Si/ Al ratio by year

6. Conclusions and path forwards

This paper provides an overview of the progress in the beryllium brazing project. Thermodynamics turned out to be an excellent tool in the early stages of this re-design process. This analysis provided information to make quantitative decisions for which materials to pursue. Tests conducted to support the theoretical findings were executed within the CFM production environment. This direct approach increases data reliability and speeds up the design process.



Relevant process variables, braze properties, braze requirements and customer requirements were addressed in the project. Certain considerations such as reactor corrosion impact on the braze material and maximum temperature during reactor upset situations still needs to be addressed. The CFM engineering department is developing new brazing equipment, based on the insight gained by this study. Currently, a design of experiments is being scheduled to further establish empirical relationships between Braze-joint properties and process variables. These empirical models will supply insight into the kinetics of the brazing process.

As previously mentioned, beryllium has an excellent record over the past 40 years of reactor operation. Al will be further pursued as an alternative material depending on how it affects the braze properties with a possibility of hydrogen/deuterium uptake. The next option is to pursue other brazing alloys which contain de-oxidizers as listed in section 4.2. Within this project, further testing of a CuBe-alloy will be investigated. Recently, the CANDU Owners Group (COG) started a comprehensive study with other investigators (i.e., Atomic Energy of Canada Limited and other fuel manufacturers) to investigate this issue with the participation of CFM and RMC in order to build and expand upon the current work.

7. References

- [1] D.R.Olander, "General Thermodynamics", CRC Press Taylor & Francis group, 2008
- [2] K.A.Welsh, "Beryllium Chemistry and Processing", ASM International, July 2009
- [3] R.D.Weir and Th.W.de Loos, "Measurement of the Thermodynamic properties of multiple phases", IUPAC Chemical data series, 2005
- [4] H.Okamoto, L.E.Tanner and J.P.Abriata, "Phase Diagrams of Binary Beryllium alloys", ASM International, Metal Parts, Ohio, 1987
- [5] J.Murray, A.Peruzzi and J.P. Abriata, "The Aluminum-Zirconium System", Journal of Phase Equilibria, Vol.13 No.3, 1992
- [6] J.Olmsted III and George Williams, "Chemistry", fourth edition, Wiley & Sons Inc, 2006
- [7] Korea Atomic Energy Research Institute, website <http://atom.kaeri.re.kr>
- [8] R.G.Cooper, "Winning at new products- Accelerating the process from idea to launch", Persus publishing Cambridge, Massachusetts, March 2001
- [9] Committee on Beryllium Alloy Exposures, Committee on Toxicology, "Health Effects of Beryllium Exposure: A Literature Review", National Research Council, 2007
- [10] J.G.Harmsen, Thermodynamic Computations Supportive of Brazing Zirconium Alloys, June 2010